The High Energy Resolution View of Ionized Absorbers in AGN

Fabrizio Nicastro
Harvard-Smithsonian Center for Astrophysics, 60 Garden Street, Cambridge, MA 02138

Fabrizio Fiore
Osservatorio Astronomico di Roma, Via dell'Osservatorio 2, Monteporzio Catone (Rm), I-00040 Italy

Giorgio Matt
Universitá degli Studi "Roma-Tre", Via della Vasca Navale 84, I-00146, Roma, Italy

ABSTRACT

A number of emission and absorption features are expected to be visible in high energy resolution X-ray spectra of type 1 AGN with ionized gas along the line of sight (so called "warm absorbers"). Emission strongly depends on the geometrical configuration of the gas, while absorption along the line of sight does not. Absorption features include photoelectric absorption K and L edges along with many strong Kα, Kβ and L resonance absorption lines from the most abundant elements. We present detailed simulations of our "photoelectric + resonant absorption" model with the high energy resolution gratings and calorimeters of AXAF, XMM and Constellation-X, and discuss the relevant physics which can be addressed with the new generation of X-ray spectrometers.

1. Introduction

In about 50% of flat X-ray spectrum, broad optical emission line, type 1 AGN, ionized matter along the line of sight absorbs the nuclear X-ray continuum (Reynolds et al., 1997, George et al., 1998). Main signatures in the transmitted soft X-ray spectra of these AGN are deep and broad K absorption edges, mainly from highly ionized Oxygen and Neon, but a number of other weaker and/or narrower absorption features are predicted by photoionization and collisional ionization models, including Iron L edges, and more than 200 strong K and L resonance absorption lines from C, O, Ne, Mg, Si, S and Fe (Nicastro et al., 1998a). Emission features are also predicted, with intensities and equivalent widths highly depending on the geometry. Moreover, these would be the only spectral features revealing the presence of this component if the line of sight was not obscured by the ionized gas (see also Matt, 1998, this conference).

However photoionization models predict quite low emission and absorption line intensities and equivalent widths, with the latter ranging from ~ 1 to ~ 10 eV depending on the geometry and the gas dynamics. (Netzer, 1993, 1996, Nicastro, Fiore & Matt, 1998a, Matt, 1998, this conference).

For this reason moderate resolution soft X-ray spectrometers ($\Delta E = 0.1$ keV @ 1keV), have so far permitted only the detection and marginal separation of the OVII and OVIII absorption K edges at 0.74 and 0.87 keV respectively (the strongest predicted absorption features). This has allowed estimates of the mean ionization degree and column density of the "warm" gas (Reynolds et al., 1997).

Many more questions concerning the physical state, the geometry and the source of ionization of the gas are still open, and unambiguous answers can be found only by the next generation of X-ray spectrometers, with greatly improved energy resolution. In this work we present our "Photoelectric+Resonant Absorption" model (Nicastro, Fiore & Matt, 1998a), and show its diagnostics capability in conjuction with high resolution, high collecting area X-ray spectra of AGN, as will be available with the next generation of X-ray gratings and calorimeters onboard AXAF, XMM and Constellation-X.

2. Models

Details of our model are described in Nicastro et al. (1998a, 1998b). We present here two spectra transmitted from single outflowing (v=1000 km s^{-1}) clouds of photoionized and collisionally ionized gas respectively. The "turbulence" velocity is $\sigma_v = 1000$ km s^{-1} (note that we have not included emission line spectra, since these are highly geometry dependent). The column density in both cases is fixed at 10^{22} cm^{-2} (a commonly observed value, Reynolds, 1997) and we adopt an ionization parameter (LogU=0.1) and an electron temperature (LogT_e=6.5) such that, in both cases, the relative ionic abundances of OVII and OVIII are similar. We adopt a small covering factor (as seen from the central source) of $\Omega/4\pi = 10^{-2}$. This allows us to neglect the contribution of the gas emission. The 0.1-2.5 keV flux is 2.6×10^{-11} erg s^{-1} cm^{-2}, corresponding to a ROSAT-PSPC count rates of 2.5 ct/s, similar to that observed from the brightest Seyfert 1 nuclei (e.g. NGC 3516, Mathur et al., 1997). Fig. 1 shows these two transmitted spectra. The main resonance absorption lines are labeled in both panels. The different line ratios in the two cases are mainly due to the broader ionizing photon distribution (a multi-power law) in the photoionization case, compared with the narrow electron temperature distribution (a maxwellian) in the collisional case (Nicastro et al., 1998b).

3. Simulations

The new generation of X-ray spectrometers will offer the opportunity to detect and separate narrow ($\sim 1-2$ eV) absorption features. We built a simple "simulator" to fold our models with the responses of (a) the AXAF-Medium Energy Grating (AXAF-MEG: $\Delta E = 1.5$ eV, collecting area = 100 cm^2 @ 1 keV, "AXAF Proposer's Guide", vs 1.0, 1997); (b) the XMM-Reflecting Grating Spectrometer (XMM-RGS 1st order: $\Delta E = 3.5$ (1.5 in 2nd order) eV, collecting area

~ 500 (200 in 2nd order) cm^2 @ 1 keV); and (c) the baseline Constellation-X calorimeter ($\Delta E = 3$ eV, collecting area $\sim 10,000$ cm^2 @ 1 keV, "The High Throughput X-ray Spectroscopy (HTXS) Mission", 1997). We added statistical (and instrumental, when available) noise. Fig. 2 shows the 80 ks XMM-RGS simulation (the intermediate case, as far as the collecting area is concerned). Spectra of such and even better signal to noise will be possible for all the known Seyfert 1 galaxies with "warm absorber". Spectra of comparable quality can be obtained for source with 2-10 flux down to $\sim 5 \times 10^{-12}$ erg s^{-1} cm^{-2} (~ 600 targets). Fig. 3 shows a particular of AXAF-MEG and XMM-RGS (1st and 2nd order) simulations of the same model of Fig. 1 (upper panel), for two values of the "turbulence" velocity $\sigma_v = 200$ and 1000 km s^{-1}. The bottom panel of this figure shows the same particular for a 20 ks Constellation-X simulation and for the case $\sigma_v = 200$ km s^{-1}.

The factor of ~ 6 larger collecting area of XMM-RGS, compared to AXAF-MEG, will allow detailed spectral variability studies of warm absorbers in bright AGN significantly changing their intensity state on timescales of $\gtrsim 50$ ks (e.g. NGC 5548). Fig. 4 show this capability for two spectra emerging from gas in photoionization equilibrium with ionizing continua differing by a factor 2 in intensity.

4. Diagnostic

The optical depth $\tau^{X^i}_{\nu_0^{j\to k}}$ of the resonance absorption line due to the $j \to k$ transition of the ion i of the element X, at the core frequency $\nu_0^{j\to k}$ is given by the product between the total optical depth and the Voigt profile at the core frequency: $\tau^{X^i}_{\nu_0^{j\to k}} = \tau_T \phi_{\nu_0^{j\to k}}$. The total optical depth depends linearly on (a) the chemical composition A_X, (b) the relative ionic abundance n^i_X, (c) the equivalent hydrogen column density N_H, and (d) the oscillator strength $f^{X^i}_{j\to k}$:

$$\tau^{X^i}_{\nu_0^{j\to k}} = \tau_T \phi_{\nu_0^{j\to k}} = \left(A_X n^i_X N_H f^{X^i}_{j\to k} \right) \times \phi_{\nu_0^{j\to k}} \tag{1}$$

A measure of both the optical depth and the relative intensity at the center of two observed lines produced by two ions of a same element may then allow for an estimate of the relative ionic abundances. This in turn allows (a) for unambiguously distinguishing between photoionization and collisional ionization (see Table 1, col. II, "phot. vs coll"), and (b) for a stringent test of time-evolving non equlibrium photoionization model (see Fig. 4, lower panel). Furthermore, the measure of the ratio between two lines due to two transition of the same ion of the same element, will permit to estimate the chemical composition of the gas. Finally, the position of the line and its width can give us information on the dynamical state of the gas. Accurate measure of blueshift or redshift of the absorption lines will allow to estabilish if the gas is outflowing or inflowing respectively. Furthermore line widths greater than predicted by the only thermal motion of the ions will permit to estimate the degree of turbulence of the gas along the line of sight (e.g. NeIX, NeX, see Fig. 4).

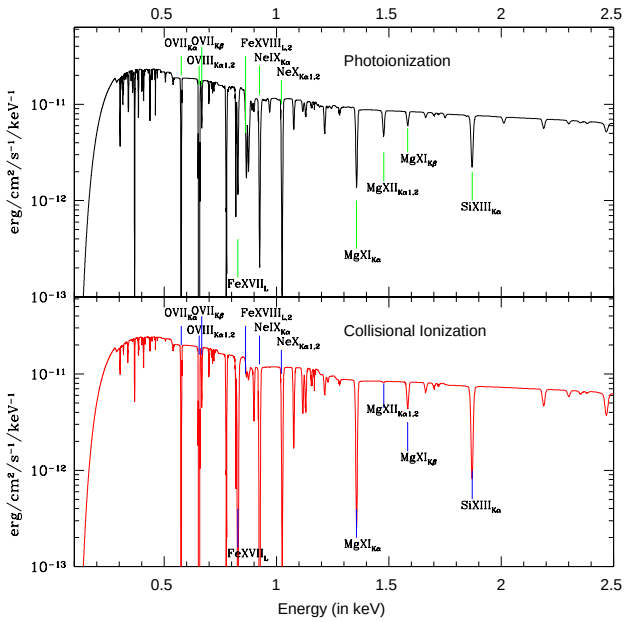

Fig. 1.— Spectra emerging from a cloud of outflowing and turbulent ionized gas in photoionization (upper panel) and collisional ionization (lower panel) equilibrium. Absorption by a column of 3×10^{20} cm^{-2} neutral gas has been included, to account for Galactic absorption.

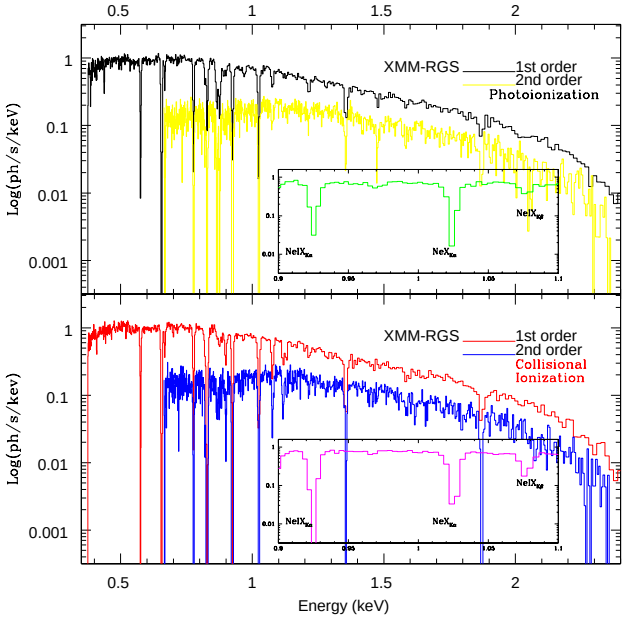

Fig. 2.— 80 ks XMM-RGS, 1st and 2nd order order simulations of the models in the upper and lower panels of Fig. 1 (upper and lower panels respectively). Internal windows show the 0.9-1.1 keV portion of the simulated spectra.

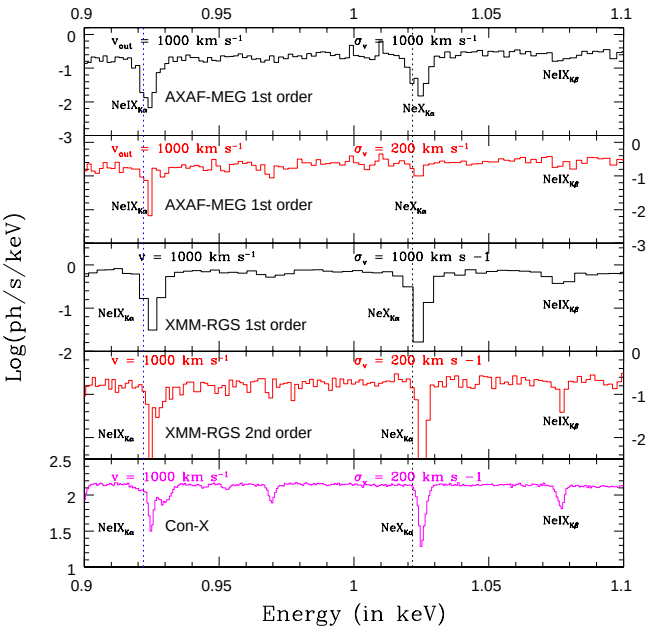

Fig. 3.— 0.9-1.1 keV portion of AXAF-MEG (first and second panels), XMM-RGS 1st and 2 order (third and fourth panel) and Constellation-X (5th panel) simulations of the model in the upper panel of Fig. 1. The dashed, blue vertical line in all the panels indicates the rest energies of the NeIXKα and the NeXKα lines.

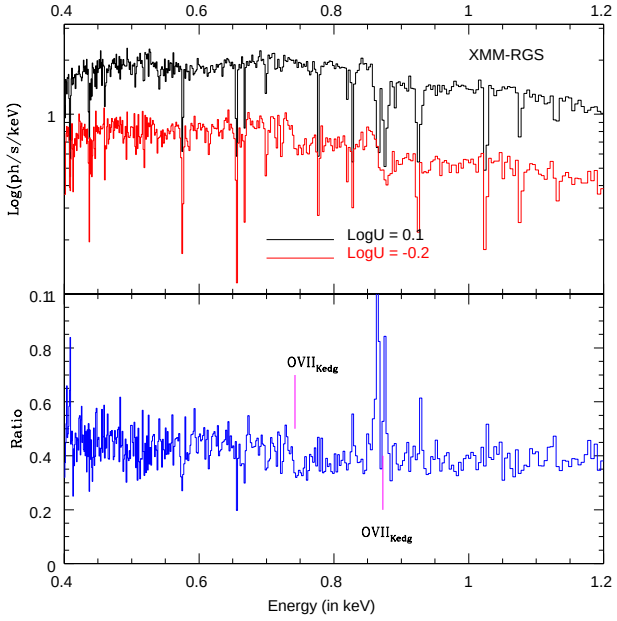

Fig. 4.— 80 ks XMM-RGS simulations of two spectra emerging from a cloud of gas in photoionization equilibrium with two ionizing continua differing by a factor of 2 in intensity (upper panel). The lower panel shows the ratio ("Low" over "High" state) between these two emerging spectra.

Table 1: Relative ionic abundances, outflowing and turbolence velocity

	Model Predictions	AXAF-MEG	XMM-RGS	Constellation-X
$(n_{OVIII}/n_{OVII})_{ph}$	8.78	—	9.1 ± 0.8	8.75 ± 0.05
$(n_{OVIII}/n_{OVII})_{col}$	7.20	—	8.0 ± 1.0	7.22 ± 0.05
$(n_{NeX}/n_{NeIX})_{ph}$	1.97	1.7 ± 0.4	2.0 ± 0.2	1.98 ± 0.02
$(n_{NeX}/n_{NeIX})_{col}$	0.50	0.6 ± 0.1	0.50 ± 0.07	0.49 ± 0.02

[a] In km s^{-1}. Both the outflowing and the turbulence velocities are calculated by using the NeIX and NeX Kα lines.

[b] Calculated using the 2nd order simulated XMM-RS spectra.

We use the data simulated with the AXAF-MEG, the XMM-RGS (1st and 2nd order) and the Constellation-X calorimeter to measure some of the above quantities, and present the results in Table 1. The model parameters are those described in §2, except for the turbulence velocity which is here $\sigma_v = 200$ km s^{-1}.

REFERENCES

Mathur S., Wilkes B.J. & Aldcroft T., 1997, ApJ, 478, 182.

George I.M., Turner T.J., Netzer H., Nandra K., Mushotzky R.F., & Yaqoob T., 1998, ApJS, 114, 73

Netzer H., 1993, ApJ, 411-594

Netzer H., 1996, ApJ, 473, 781

Nicastro F., Fiore F., Matt G., 1998a, ApJ, submitted.

Nicastro F., Fiore F., Perola G.C. & Elvis M., 1998b, ApJ, in press, astro-ph/9808316.

Reynolds C.S., 1997, MNRAS 287, 513.